Supporting Information

Microporous Metal-Organic Framework Stabilized by Balanced Multiple Host-Couteranion Hydrogen Bonding Interactions for High-density CO_2 Capture at Ambient Conditions

Yingxiang Ye,[a] Shunshun Xiong,[b] Xiaonan Wu,[b] Liuqin Zhang,[a] Ziyin Li,[a] Lihua Wang,*[a] Xiuling Ma,[a] Qian-Huo Chen,[a] Zhangjing Zhang,[a,c] and Shengchang Xiang,*[, a,c]

[a] *College of Chemistry and Chemical Engineering, Fujian Provincial Key Laboratory of Polymer Materials, Fujian Normal University, 32 Shangsan Road, Fuzhou 350007, P R China Corresponding Author E-mails: L. Wang (lhwang@fjnu.edu.cn) and S. Xiang (scxiang@fjnu.edu.cn)*

[b] *Institute of Nuclear Physics and Chemistry, China Academy of Engineering Physics, Mianyang, Sichuan, 621900, P R China.*

[c] *State Key Laboratory of Structural Chemistry, Fujian Institute of Research on the Structure of Matter, Chinese Academy of Sciences, Fuzhou, Fujian 350002, PR China*

Contents

Experimental Section

Chemicals: Thionyl chloride ($SOCl_2$), hydrazine hydrate ($N_2H_4 \cdot H_2O$, 85%), diethyl ether, o-xylene, 4-aminobenzoic acid and N, N'-dimethylformamide (DMF), were purchased from Shanghai Chemical Reagent Co. All starting materials were used without further purification. The ligand Hcpt was prepared according to a known modified method.[1]

Synthesis of N,N'-Dimethylformamide Azine Dihydrochloride (DMAZ):

Thionyl chloride ($SOCl_2$, 28.6 mL, 0.4 mol) was added with stirring to DMF (150 mL) at 5 ^oC. After addition keep this mixture at 5 ^oC for 24 h and then added slowly aqueous hydrazine hydrate (5 mL, 0.1 mol) in 20 ml DMF. After addition the mixture was stirred at room temperature (rt) for 48h and the white precipitate of N, N'-dimethylformamide azine dihydrochloride was collected by filtration and washed with DMF and diethyl ether: 19.1 g (91%). (Caution: all operations involving above solvent should be conducted in a fume hood.)

Synthesis of 4-(4H-1,2,4-Triazol-4-yl)benzoic Acid (Hcpt)

Refluxing a mixture of N, N'-dimethylformamide azine dihydrochloride (2 g, 9.33 mmol) and 4-aminobenzoic acid (1.28 g, 9.33 mmol) in 25 ml o-xylene (reaction should be conducted in a fume hood) for 24 h gave a pale yellow solid, which was filtered and washed with EtOH (1×10 mL) and Et_2O (1×8 mL); yield: 1.21 g (69%). Furthermore, the pale yellow solid and water (5 mL) were transferred into a parr Teflon-lined stainless steel vessel (23.0 mL) and heated to 150 ^oC for 24 h under autogenous pressure, and cooled to room temperature at a rate of 5.0 °C h^{-1}. Colorless rod-shaped crystals of Hcpt suitable for single crystal x-ray analysis were obtained directly.

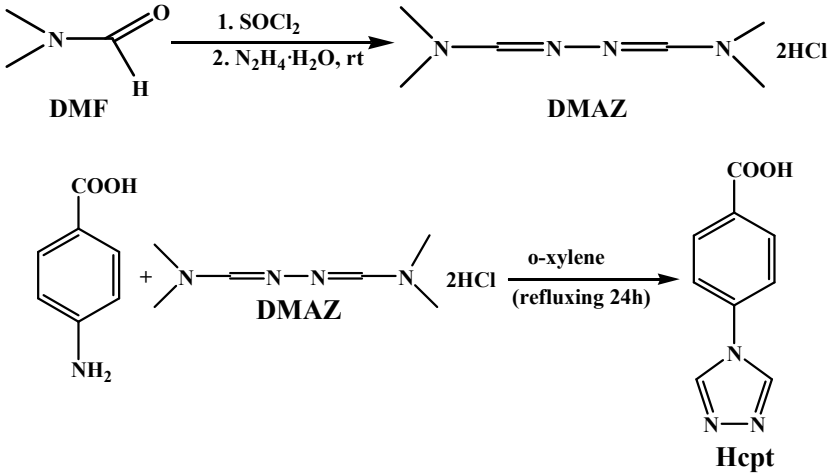

Scheme S1. Synthesis of DMAZ and 4-(4H-1,2,4-Triazol-4-yl)benzoic Acid (Hcpt).

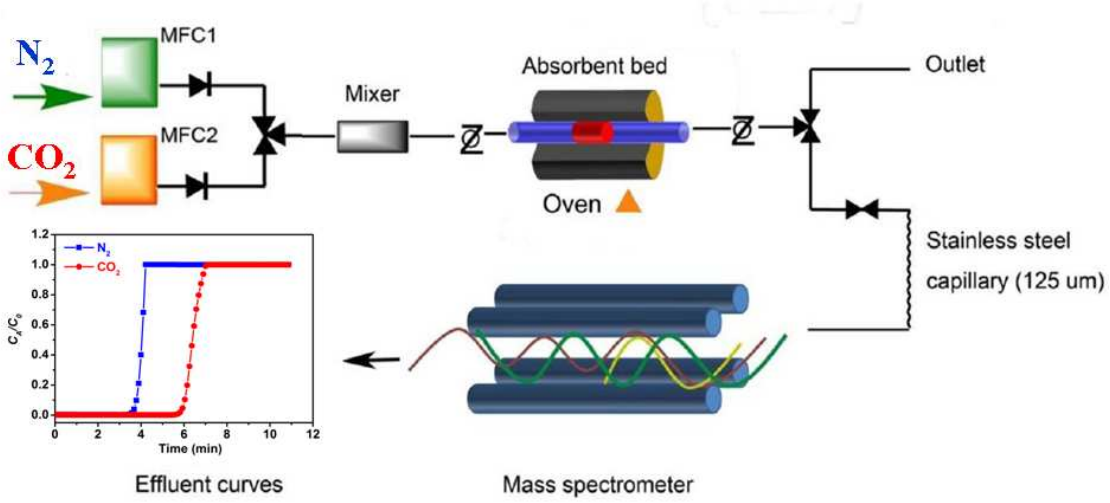

Scheme S2. Illustration of a lab-scale fix-bed reactor.

Table S1 | Crystallographic Data and Structural Refinement Summary.

Compounds	**FJU-14-NO_3**	**FJU-14-ClO_4**	**FJU-14-BF_4**	**FJU-14-BF_4-a**	**FJU-14-BF_4-a·0.93 CO_2**
CCDC	1426056	1426057	1426058	1426059	1426060
Empirical formula	$C_{36}ClCu_4N_{15}O_{21}H_{32}$	$Cu_4Cl_4C_{36}N_{12}O_{24}H_{32}$	$Cu_4ClB_3C_{36}F_{12}N_{12}O_{12}H_{32}$	$Cu_4ClB_3C_{36}F_{12}N_{12}O_{12}H_{32}$	$Cu_4ClB_3C_{36.93}F_{12}N_{12}O_{13.86}H_{32}$
Formula weight	1300.37	1412.71	1374.77	1374.77	1415.69
Temperature (K)	150	150	150	150	100
Crystal system	tetragonal	tetragonal	tetragonal	tetragonal	tetragonal
Space group	*I4/mmm*	*I4/mmm*	*I4/mmm*	*I4/mmm*	*I4/mmm*
a (Å)	13.9585(4)	14.2066(2)	14.1125(5)	14.1245(7)	14.0241(7)
b (Å)	13.9585(4)	14.2066(2)	14.1125(5)	14.1245(7)	14.0241(7)
c (Å)	20.0529(8)	19.8137(4)	19.8583(7)	19.9049(10)	19.9373(11)
α (°)	90	90	90	90	90
β (°)	90	90	90	90	90
γ (°)	90	90	90	90	90
Volume ($Å^3$)	3907.1(3)	3998.92(14)	3955.1(3)	3971.1(4)	3921.2(4)
Z	2	2	2	2	2
D_c (g cm^{-3})	1.098	1.167	1.148	1.143	1.192
μ (mm^{-1})	2.066	2.974	2.184	2.176	2.237
F(000)	1292.0	1400.0	1352.0	1352.0	1393.0
Crystal size (mm^3)	0.3×0.25×0.2	0.25×0.25×0.2	0.2×0.2×0.15	0.2×0.15×0.15	0.2×0.15×0.15
Radiation	Cu *Kα* (λ =1.54184Å)	Cu *Kα* (λ =1.54184Å)	Cu *Kα* (λ =1.54184Å)	Cu *Kα* (λ =1.54184Å)	Cu *Kα* (λ =1.54184Å)
Goodness-of-fit on F^2	1.079	1.079	1.081	1.061	1.087
Final *R* indexes [*I*>=2σ (*I*)][(a)]	R_1=0.0494, wR_2 = 0.1432	R_1 = 0.0966, wR_2 = 0.2861	R_1 = 0.0677, wR_2 = 0.1920	R_1 =0.1123 wR_2 = 0.3262	R_1 =0.0936, wR_2 = 0.2499
Final R indexes [all data] [(a)]	R_1 = 0.0527, wR_2 =0.1461	R_1 = 0.0982, wR_2 =0.2886	R_1 = 0.0808, wR_2 = 0.2068	R_1 =0.1215, wR_2 = 0.3538	R_1 =0.1066, wR_2 = 0.2703

$(a)\ R_1 = \sum||F_O| - |F_c|| / \sum|F_O|; wR_2 = [\sum w(|F_O|^2 - |F_c|^2)^2 / \sum w(F_O^2)^2]^{1/2}$

Table S2 | The comparison of CO_2 adsorption performances on **FJU-14-BF_4-a** with representative MOFs.

Compounds	CO_2 uptake 296 K, 1 bar		Functional sites	BET (m^2/g)	Q_{st} (kJ/mol)	V_p^j (cm^3/g)	ρ^l (g/cm^3)	ref
	cm^3/cm^3	cm^3/g						
FJU-14-BF_4-a	95.8	83.6	BF_4, H_2O	324	18.8[i]	0.172	0.955	This work
Cu(bpy-2)$_2$(SiF_6)	41	61.5	SiF_6	2718	21[i]	1.143	0.106	2
SIFSIX-2-Cu	26	41.4	SiF_6	3140	22[i]	1.166	0.070	3
TIFSIX-1-Cu	91.6	106.3	TiF_6	1690	26.5[i]	0.664	0.314	4
SNIFSIX-1-Cu	89.0	93.9	SnF_6	1523	26.5[i]	0.572	0.322	4
Cu(bpy-1)$_2$(SiF_6)	99.0	115.2	SiF_6	1468	27[i]	0.656	0.345	2
PCN-88	81.5	123.2	OMS[b]	3308	27[i]	1.599[k]	0.151	5
UTSA-48	22.1	28	SiF_6, LBS[c]	285	30[i]	0.208	0.264	6
MOF-253 -0.97Cu(BF_4)$_2$	NA[a]	62	BF_4, OMS	705	30[h]	0.386	0.316	7
SIFSIX-2-Cu-i	151	121.2	SiF_6	735	31.9[i]	0.324	0.735	3
UTSA-16	160	96.9	H_2O	628	34.6[i]	0.310	0.614	8
Cu-BTC	82.3	93.8	OMS	1734	35[g]	0.848	0.217	9
Cu-TDPAT	103	131.6	OMS,LBS	1938	42[i]	0.930	0.278	10
Mg_2(dobpdc)	102	144	OMS	3270	44[d]	1.384	0.204	11
MPM-1-TIFSIX	115.7	89.6	TiF_6,LBS	840	44.4[i]	0.402	0.438	12
Bio-MOF-11	113	91.8	OMS,LBS	1040	45[e]	0.450	0.401	13
SIFSIX-3-Zn	90	57	SiF_6	250	45[i]	NA	NA	3
MgMOF-74	162	179.5	OMS	1800	47[f]	0.572	0.616	14
MAF-35	135.5	99.9	OMS	974	47[d,g]	0.375	0.523	15
SIFSIX-3-Ni	NA	56	SiF_6	NA	48[i]	NA	NA	16
CAU-1	76	85	LBS	1268	48[e]	1.320	0.126	17
SIFSIX-3-Cu	NA	56.4	SiF_6	300	54[i]	NA	NA	18
Mmen-CuBTTri	83	94	LBS	870	96[h]	0.353	0.523	19
[Co_2Cl_2(bbta)(OH)]	203	150	OMS,LBS	1167	110[i]	0.400	0.737	20
Cu(BF_4)$_2$(bpy)$_2$	NA	62	BF_4	622	NA	0.363	0.335	21

H_2bbta = 1H,5H-benzo(1,2-d:4,5-d')bistriazole; TIFSIX = TiF_6^{2-} anions; SNIFSIX = SnF_6^{2-} anions; bpy-1 and bpy = 4,4′-bipyridine; bpy-2 = 1,2-bis(4-pyridyl)ethane; SIFSIX = SiF_6^{2-} anions; Mmen = N,N'-dimethylethylenediamine; BTTri = 1,3,5-tris(1H-1,2,3,-triazol-5-yl)benzene; dobpdc = 4,4'-dioxido-3,3'-biphenyldicarboxylate; dobdc = 2,5-dioxido-1,4-benzenedicarboxylate; TDPAT = 2,4,6-tris(3,5-dicarboxylphenyl-amino)-1,3,5-triazine.

[a] NA = Not Available.

[b] OMS= Open Metal Sites.

[c] LBS= Lewis Basic Sites.

[d] Obtained by the Clausius-Clapeyron equation and dual-site Langmuir-Freundlich fitting.

[e] Obtained by the Clausius-Clapeyron equation and single-site Langmuir-Freundlich fitting.
[f] Obtained by the Clausius-Clapeyron equation and Toth fitting.
[g] Obtained by the Clausius-Clapeyron equation without mathematical fitting.
[h] Obtained by the Clausius-Clapeyron equation and dual-site Langmuir fitting.
[i] Obtained by the Virial fitting method.
[j] Pore volume V_p ($cm^3\ g^{-1}$) calculated from N_2 sorption isotherm at 77 K.

$$V_p = \frac{N_{\max(N_2,77K)} \times 28}{22.4 \times 0.809 \times 1000} \qquad (6)$$

[k] Pore volume V_p ($cm^3\ g^{-1}$) calculated from CO_2 sorption isotherm at 196 K.

$$V_p = \frac{N_{\max(CO_2,196K)} \times 44}{22.4 \times 1.032 \times 1000} \qquad (5)$$

[l] Calculated the density of loaded CO_2 by the equation

$$\rho = \frac{N_{(CO_2)} \times 44}{V_p \times 22.4 \times 1000} \qquad (7)$$

Where V_p is the calculated pore volume of the MOF samples ($cm^3\ g^{-1}$), $N_{\max(CO_2,196K)}$ is CO_2 sorption capacity at 196 K and 1 bar ($cm^3\ g^{-1}$); $N_{\max(N_2,77K)}$ is N_2 sorption capacity at 77 K and 1 bar ($cm^3\ g^{-1}$); ρ is the density of loaded CO_2 (g cm^{-3}), and $N_{(CO_2)}$ is CO_2 sorption capacity at 296 K and 1 bar ($cm^3\ g^{-1}$).

Table S3 | Summary of the parameters and the enthalpy of gas adsorption on **FJU-14-BF_4-a** at 296 and 273 K obtained from the virial equation.

Sample	adsorbate	T/K	A_0/ ln(mol g^{-1} Pa^{-1})	A_1/ g mol^{-1}	R^2	K_H/ mol g^{-1} Pa^{-1}	ΔH/ kJ mol^{-1}
FJU-14-BF_4-a	CO_2	296	-16.171	-242.933	0.998	9.485×10^{-8}	18.8
		273	-15.525	-277.003	0.999	1.810×10^{-7}	

Table S4 | The multiple hydrogen bonding interactions between the counter anions and cationic frameworks in **FJU-14**.

Compounds	Contacts	D···A (Å)	D-H···A (°)	A···H (Å)
FJU-14-NO_3	Ow···O3	2.742		
	C4-H4···O2	3.459	139.07	2.702
	C3-H3···O2	3.016	148.76	2.182
FJU-14-ClO_4	Ow···O3	3.527		
	C6-H6···O4	3.142	157.88	2.261
FJU-14-BF_4	Ow···F1	3.466		
	C1-H1···F2	3.133	159.24	2.246
FJU-14-BF_4-a	Ow···F1	3.219		
	C1-H1···F2	3.258	163.38	2.356

Table S5 | The multiple-point supramolecular interactions between the CO_2 molecules and the frameworks in **FJU-14-BF_4-a·0.93CO_2**.

Sites	Contacts	d (Å)
CO_2-I	(CO_2) O3···C6 (triazolyl)	3.031
CO_2-II	(H_2O) Ow···C7 (CO_2)	2.065
	(BF_4^-) F1···O4 (CO_2)	2.191

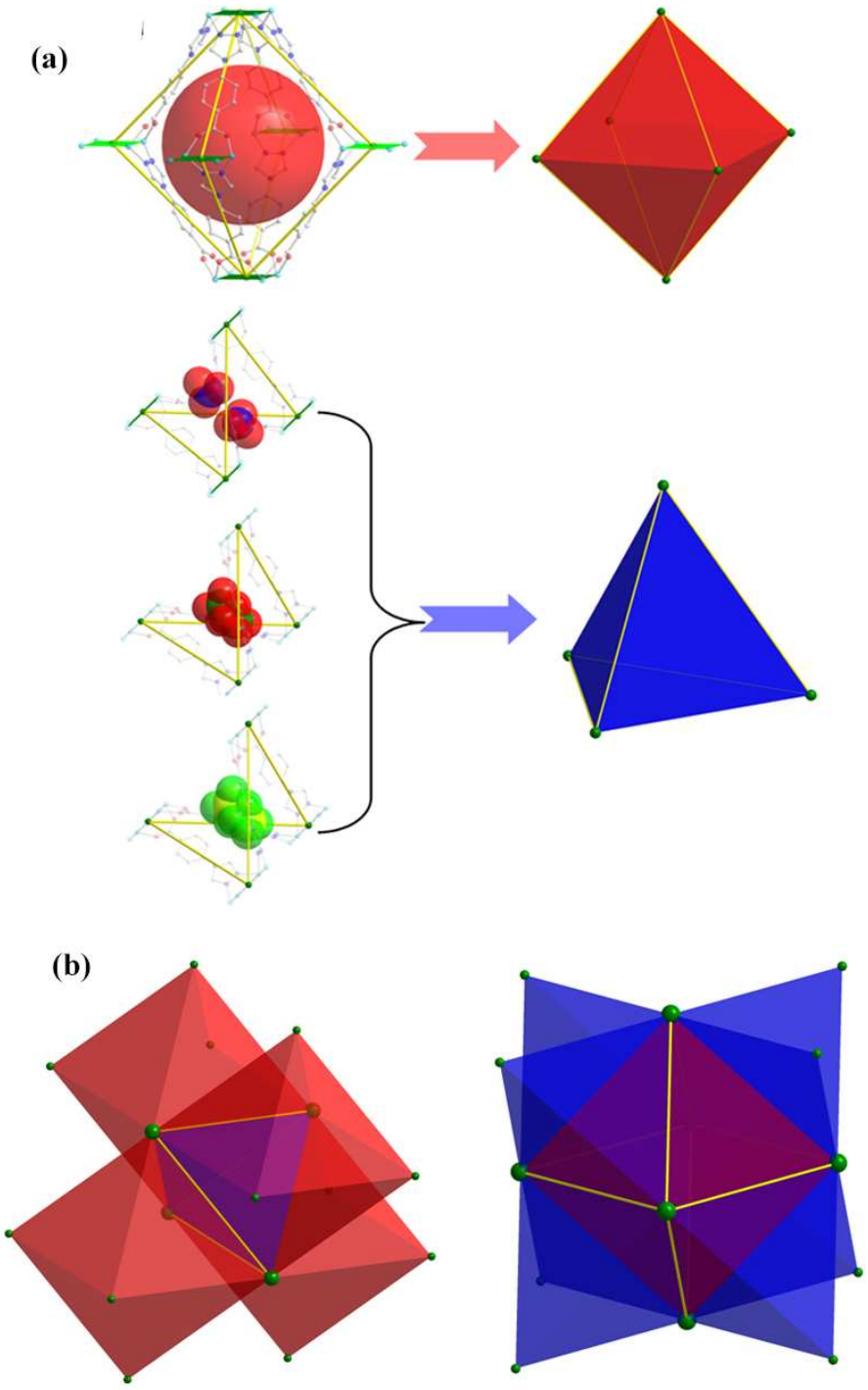

Figure S1 | (a) The structure of the octahedral (red) and tetrahedral (blue) cages (The hydrogen atoms are omitted from the structure for clarity) in **FJU-14**. (b) Cage-A is linked by eight Cage-B through sharing eight triangle faces and Cage-B is linked by four Cage-A by sharing four triangle faces.

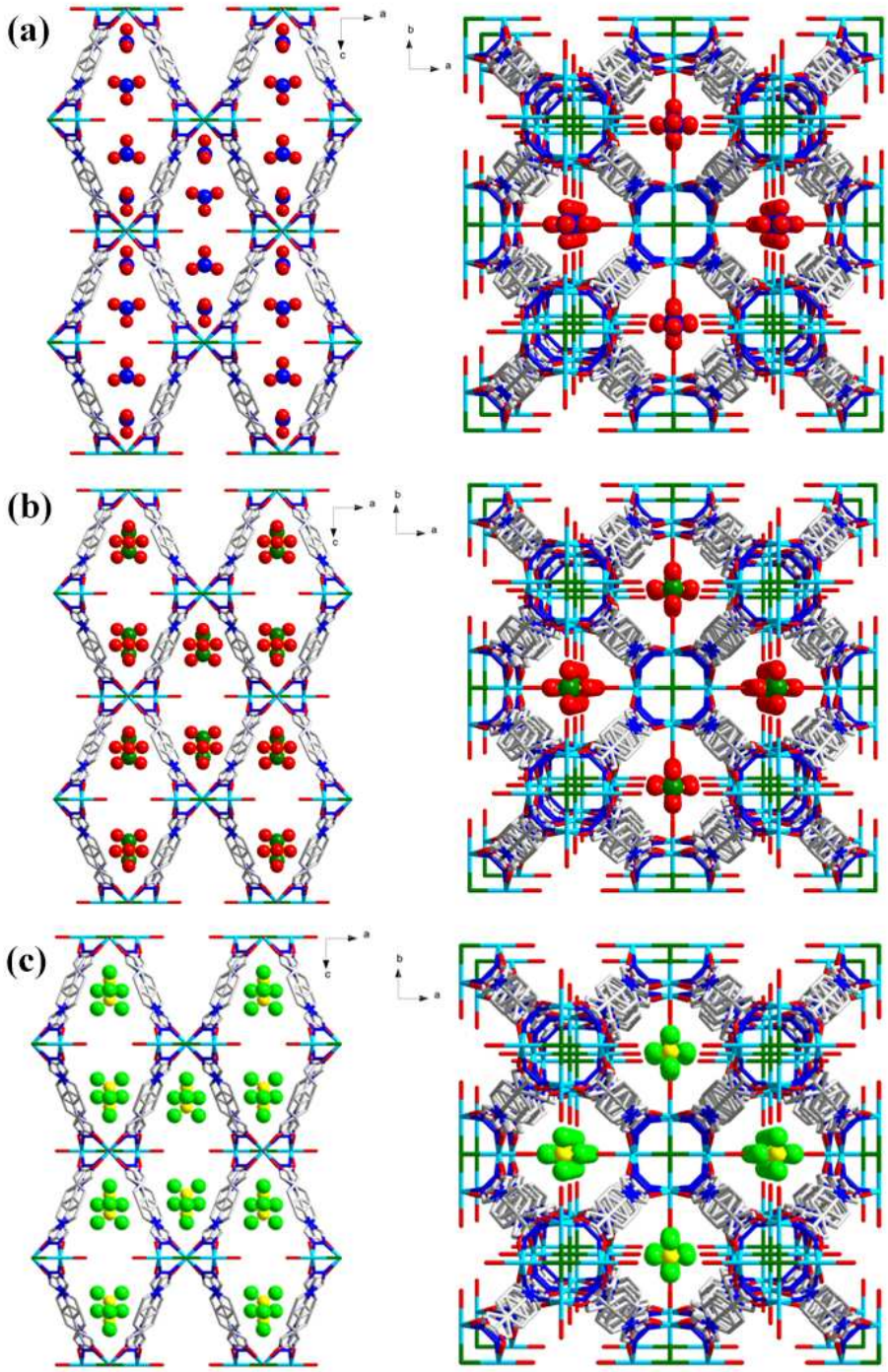

Figure S2 | The schematic representation of the (a) NO_3^-, (b) ClO_4^- and (c) BF_4^- locate □in three-dimensional cationic frameworks of **FJU-14**.

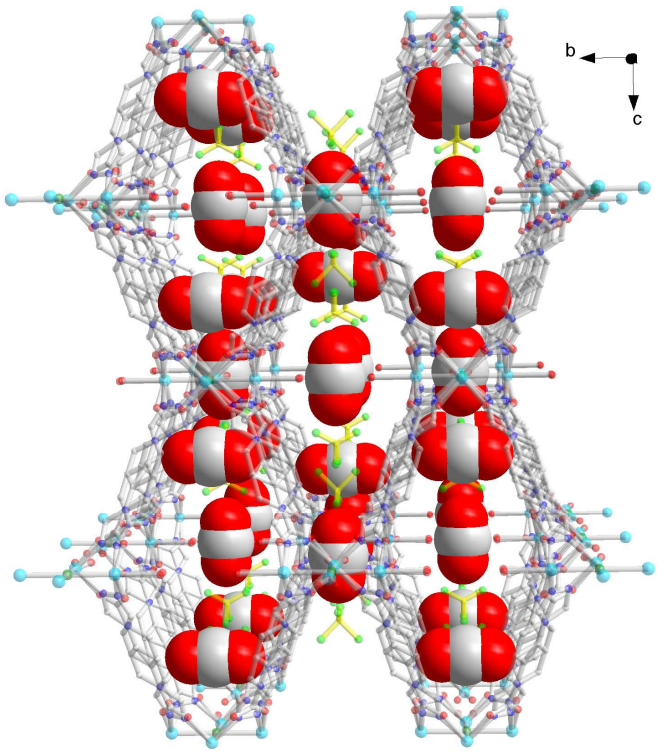

Figure S3 | The schematic representation of the CO_2 molecules locate in **FJU-14-BF_4-a·0.93CO_2**. (The hydrogen atoms are omitted from the structure for clarity)

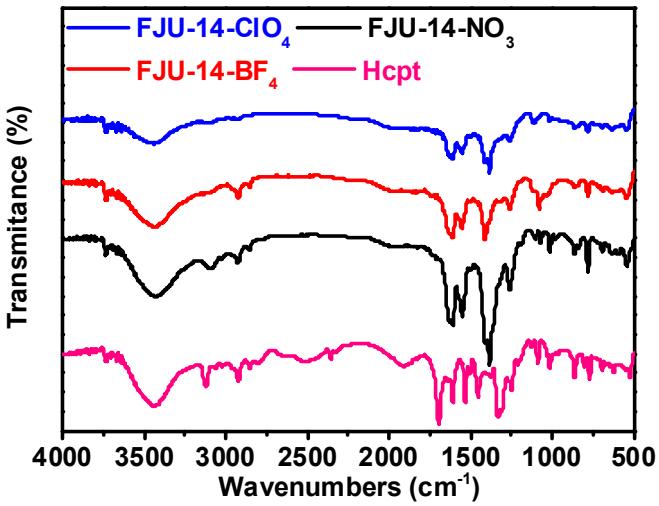

Figure S4 | IR spectra of Hcpt, **FJU-14-NO_3**, **FJU-14-ClO_4** and **FJU-14-BF_4**.

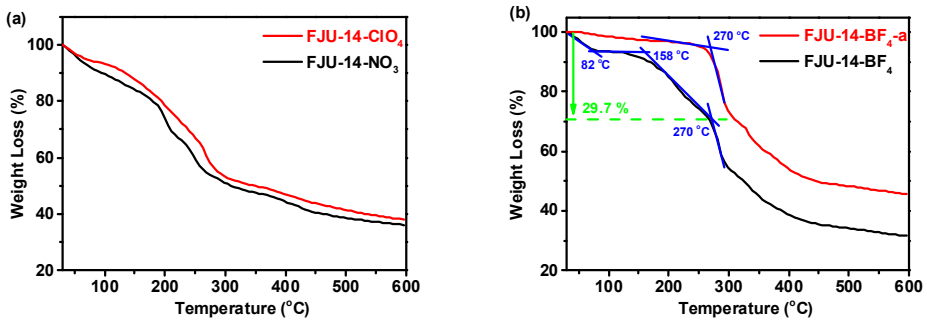

Figure S5 | The TGA curves of compounds **FJU-14-NO$_3$**, **FJU-14-ClO$_4$** (a) and **FJU-14-BF$_4$**, **FJU-14-BF$_4$-a** (b).

Thermogravimetric analyses (TGA) for the as-synthesized samples **FJU-14-NO$_3$** and **FJU-14-ClO$_4$** show a similar continuous weight loss of 30.1% and 28.2% upon heating because of the strong interaction among the high boiling point solvents and the frameworks (calcd 30.6% and 28.8%). **FJU-14-BF$_4$** shows a weight loss of 6.4% from 30 to 82 ^{o}C, corresponding to the loss of five guest H_2O and one MeOH molecules (calcd 6.6%). The weight loss of 23.3% from 158 ^{o}C to 270 ^{o}C is attributed to the loss of four lattice DMAc and four coordinated water molecules (calcd 22.8%). Further sharp weight loss occurred from 270 ^{o}C, indicating collapse of the whole frameworks.

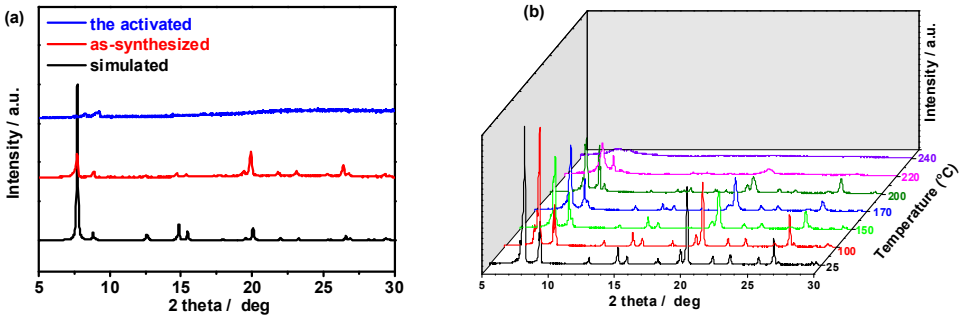

Figure S6 | (a) Room temperature conditions and (b) variable temperature powder X-ray diffraction patterns for **FJU-14-NO_3**.

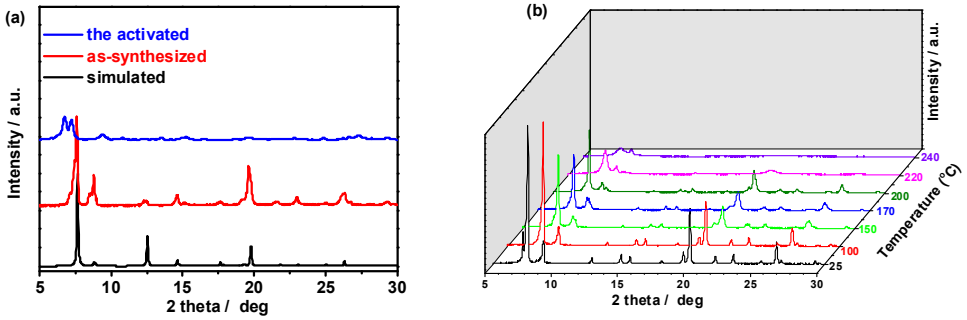

Figure S7 | (a) Room temperature conditions and (b) variable temperature powder X-ray diffraction patterns for **FJU-14-ClO_4**.

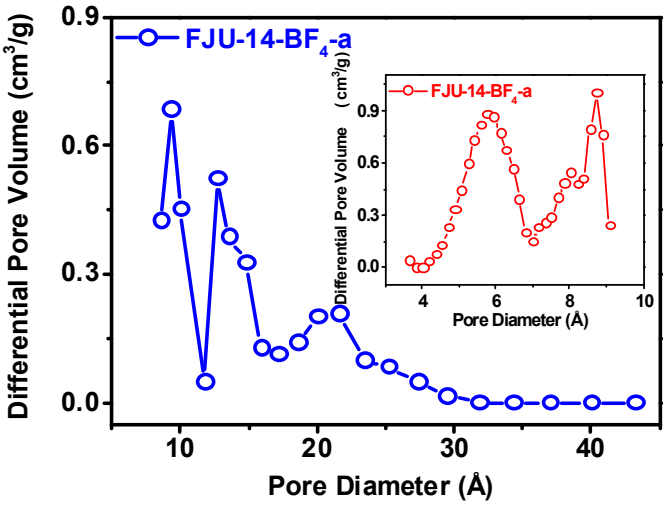

Figure S8 | Pore-size distribution for **FJU-14-BF_4-a** determined from their N_2 adsorption isotherms at 77 K calculated by using a slit/cylindrical NLDFT model. (Inset: calculated by using a slit pore NLDFT model from CO_2 adsorption at 273 K).

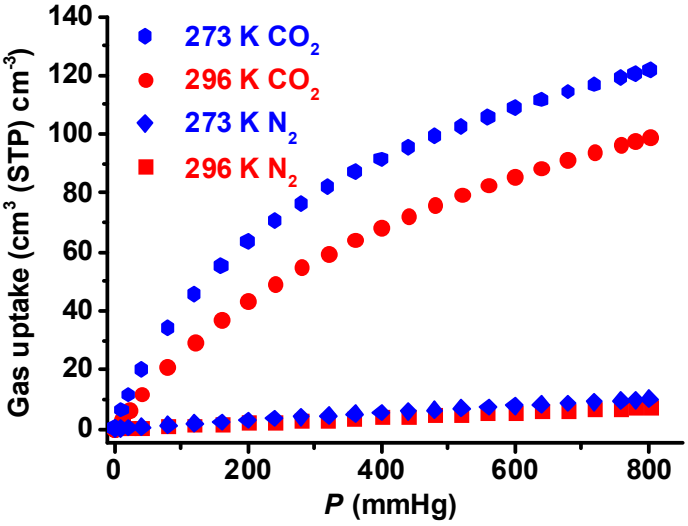

Figure S9 | CO_2 and N_2 adsorption isotherms of **FJU-14-BF_4-a** at 296K and 273 K.

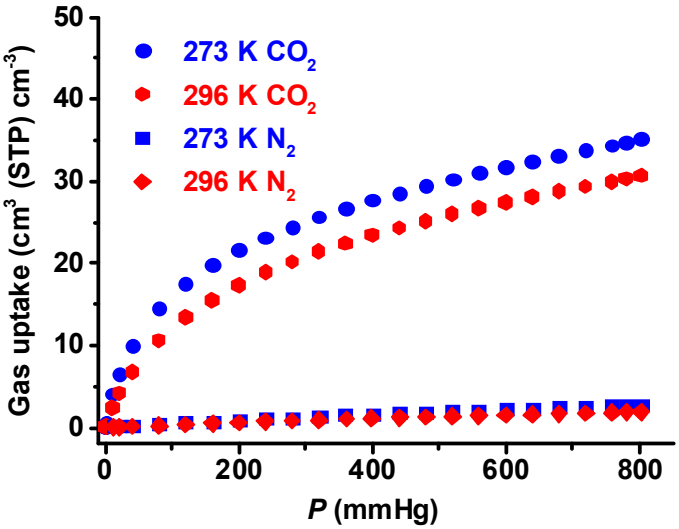

Figure S10 | CO_2 and N_2 adsorption isotherms of **FJU-14-ClO_4-a** at 296K and 273 K.

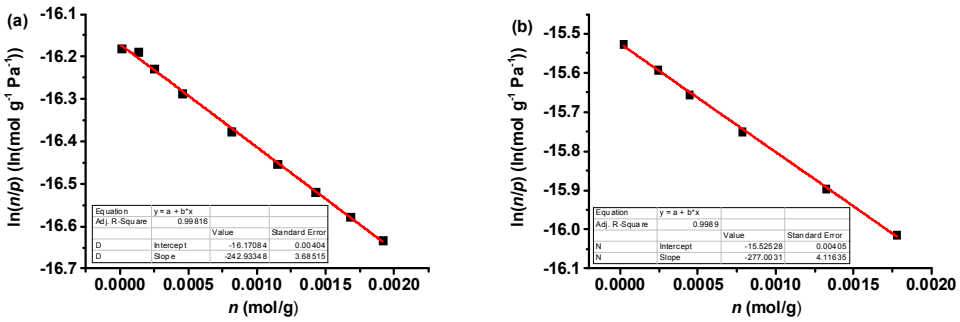

Figure S11 | The virial graphs for adsorption of CO_2 on **FJU-14-BF$_4$-a** at 296 K (a) and 273 K (b).

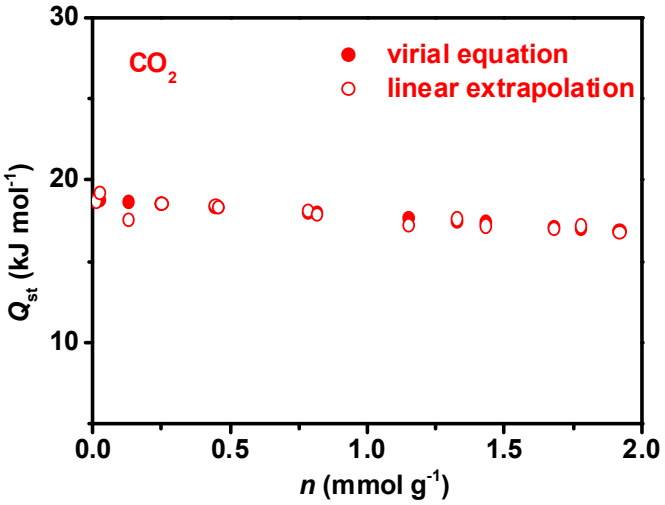

Figure S12 | Comparison of the enthalpies for gas adsorption of CO_2 on **FJU-14-BF$_4$-a** from two methods: virial equation (solid) and linear extrapolation (open).

Supplementary References

1 (a) Naik, A. D.; Marchand-Brynaer, J.; Garcia, Y. *Synthesis* **2008**, *1*, 149-154; (b) Wang, L. H.; Ye, Y. X.; Zhang, L. Q.; Chen, Q. H.; Ma, X. L.; Zhang, Z. J.; Xiang, S. C. *Inorg. Chem. Commun.* **2015**, *60*, 19-22.

2 Burd, S. D.; Ma, S.; Perman, J. A.; Sikora, B. J.; Snurr, R. Q.; Thallapally, P. K.; Tian, J.; Wojtas, L.; Zaworotko, M. J. *J. Am.Chem. Soc.* **2012**, *134*, 3663-3666.

3 Nugent, P.; Belmabkhout, Y.; Burd, S. D.; Cairns, A. J.; Luebke, R.; Forrest, K.; Pham, T.; Ma, S.; Space, B.; Wojtas, L.; Eddaoudi, M.; Zaworotko, M. J. *Nature* **2013**, *495*, 80-84.

4 Nugent, P.; Rhodus, V.; Pham, T.; Tudor, B.; Forrest, K.; Wojtas, L.; Space, B.; Zaworotko, M. *Chem. Commun.* **2013**, *49*, 1606-1608.

5 Li, J. R.; Yu, J.; Lu, W.; Sun, L. B.; Sculley, J.; Balbuena, P. B.; Zhou, H. C. *Nat. Commun*. **2013**, *4*, 1538.

6 Xiong, S.; He, Y.; Krishna, R.; Chen, B.; Wang, Z. *Cryst. Growth Des.* **2013**, *13*, 2670-2674.

7 Bloch, E. D.; Britt, D.; Lee, C.; Doonan, C. J.; Uribe-Romo, F. J.; Furukawa, H.; Long, J. R.; Yaghi, O. M. *J. Am.Chem. Soc.* **2010**, *132*, 14382-14384.

8 Xiang, S. C.; He, Y. B.; Zhang, Z. J.; Wu, H.; Zhou, W.; Krishna, R.; Chen, B. L. *Nat. Commun.* **2012**, *3*, 954-962.

9 (a) Wang, Q. M.; Shen, D. M.; Bulow, M.; Lau, M. L.; Deng, S. G.; Fitch, F. R.; Lemcoff, N. O.; Semanscin, J. *Microporous Mesoporous Mater.* **2002**, *55*, 217-223; (b) C. R.; Wade, Dincă, M. *Dalton Trans.* **2012**, *41*, 7931-7938.

10 Li, B.; Zhang, Z.; Li, Y.; Yao, K.; Zhu, Y.; Deng, Z.; Yang, F.; Zhou, X.; Li, G.; Wu, H.; Nijem, N.; Chabal, Y. J.; Lai, Z.; Han, Y.; Shi, Z.; Feng, S.; Li, J. *Angew. Chem., Int. Ed.* **2012**, *51*, 1412-1415; *Angew. Chem.* **2012**, *124*, 1441-1444.

11 McDonald, T. M.; Lee, W. R.; Mason, J. A.; Wiers, B. M.; Hong, C. S.; Long, J. R. *J. Am. Chem. Soc.* **2012**, *134*, 7056-7065.

12 Nugent, P. S.; Rhodus, V. L.; Pham, T.; Forrest, K.; Wojtas, L.; Space, B.; Zaworotko, M. J. *J. Am. Chem. Soc.* **2013**, *135*, 10950-10953.

13 An, J.; Geib, S. J.; Rosi, N. L. *J. Am.Chem. Soc.* **2010**, *132*, 38-39.

14 (a) Millward, A. R.; Yaghi, O. M. *J. Am. Chem. Soc.* **2005**, *127*, 17998-17999; (b) Caskey, S. R.; Wong-Foy, A. G.; Matzger, A. J. *J. Am. Chem. Soc.* **2008**, *130*, 10870-10871.

15 Zhou, D. D.; He, C. T.; Liao, P. Q.; Xue, W.; Zhang, W. X.; Zhou, H. L.; Zhang, J. P.; Chen, X. M. *Chem. Commun.* **2013**, *49,* 11728-11730.

16 Shekhah, O.; Belmabkhout, Y.; Adil, K.; Bhatt, P. M.; Cairns, A. J.; Eddaoudi, M. *Chem. Commun.* **2015**, *51*, 13595-13598.

17 Si, X.; Jiao, C.; Li, F.; Zhang, J.; Wang, S.; Liu, S.; Li, Z.; Sun, L.; Xu, F.; Gabelica, Z.; Schick, C. *Energy Environ. Sci.* **2011**, *4*, 4522-4527.

18 Shekhah, O.; Belmabkhout, Y.; Chen, Z.; Guillerm, V.; Cairns, A.; Adil, K.; Eddaoudi, M. *Nat. Commun.* **2014**, *5*, 4228.

19 McDonald, T. M.; D'Alessandro, D. M.; Krishna, R.; Long, J. R. *Chem. Sci.* **2011**, *2*, 2022-2028.

20 Liao, P. Q.; Chen, H.; Zhou, D. D.; Liu, S. Y.; He, C. T.; Rui, Z.; Ji, H.; Zhang, J. P.; Chen, X. M. *Energy Environ. Sci.* **2015**, *8*, 1011-1016.

21 Yang, J.; Yu, Q.; Zhao, Q.; Liang, J.; Dong, J.; Li, J. *Microporous Mesoporous Mater.* **2012**, *161*, 154-159.